



EXPERIMENTAL STUDY OF THE TENSILE STRENGTH OF OPEN-HOLE FIBER-METAL LAMINATES

Thays A. Barreto ⁽¹⁾ and **Rafael C. Santiago** ⁽²⁾

(1) Center of Engineering, Modelling and Social Sciences, Federal University of ABC, São Bernardo do Campo, SP, Brazil.

(2) Center of Engineering, Modelling and Social Sciences, Federal University of ABC, São Bernardo do Campo, SP, Brazil.

<https://doi.org/10.21452/bccm4.2018.07.03>

Abstract

Fiber-metal laminates are alternative materials for aeronautical applications because of their lightweight and high strength. However, deep study of material behaviour under field conditions is needed. One of those cases is under the presence of holes, which mark positions of rivets and fittings in a laminate plate. This work aims to define the behaviour of fiber-metal laminates with open-holes through experimental tensile tests and the use of innovative technique for measuring deformation using image correlation (DIC, Digital Image Correlation).

1. INTRODUCTION

Lots of time and efforts have been invested in the development of new materials and techniques for aircraft structural design. The goal is to find the perfect balance between strength, weight and profitability.

Result of those efforts, the fiber-metal laminates are hybrid materials, composed of thin metal layers bonded with layers of composite material [1], like GlareTM (Glass Reinforced Laminate), a combination of aluminium alloy, glass fiber and epoxy [2]. Besides being lightweight and having good fatigue resistance, the processes and techniques related to the fabrication and maintenance of Glare are very similar to those of metals [3], reducing production costs with training and new processes. Sundi and Choi [4] also highlight the material's good fire resistance, reducing the number of emergency doors needed, and good damage tolerance, reducing the number of structural components needed, the weight and the production cost of the aircraft.

Thin plates are essential elements in the aircraft structural design, not only providing covering to the structures, but also having important function in load bearing [5]. The fixation of the plates through rivets, on the other hand, implies in the presence of open-holes in the

plate, which are well-known stress concentrator factors [6], reducing the mechanical strength of the material [7] and possibly causing mechanical failure of the structure.

The open-hole tension test helps us understand the mechanical limitations of a plate containing holes like the ones described, it consists in the application of uniaxial strain to a plate containing a central hole. Because of the discontinuity represented by the hole, a region of stress concentration is formed close its edges, especially on the transversal section that cross the centre of the hole [8], the tension in these regions can get so high it may cause fractures, that's what makes this test so important.

Combining the test to the Digital Image Correlation method makes possible to document the deformation means of the material under such conditions. This technique use images captured during the whole test to measure the material local strain, defining the strain fields on the surface of an object [9]. Using the non-deformed image as reference and the Speckle Pattern technique of random painting, an algorithm divides the reference image into pre-defined areas and maps the displacement of those in the next images by looking for specific pixels.

Using both tools, this paper evaluated the behaviour of the fiber-metal laminate composed of aluminium, glass fiber and epoxy under tensile strain when containing an open-hole.

2. MATERIALS AND METHODOLOGY

The material used was FML 3/2 configuration composed of three layers of aluminium 2024-T3 and two layers of glass fiber composite at 0°/90° with epoxy, presented in Figure 1. This FML composition presents itself as a good option for aeronautical application since it has damage tolerance greater than the aluminium and the glass fiber/epoxy composite, better behaviour under fatigue, specific weight 10% smaller than the aluminium, better fire resistance and since it can be conformed and repaired using the same processes as the aluminium [2].

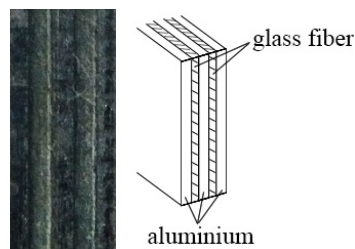


Figure 1: FML configuration tested.

Six specimens were selected for the behaviour analysis of the material plate with open-hole under tensile load, being one for characterization of the material and one as a backup, both un-notched. All the specimens tested had standard values of width (w) and thickness (t), varying only the diameter of the hole (d). It was defined a test length (L) of 100 mm to each specimen so that the stress implied in the clamping of the specimen would not interfere on the open-hole region. Table 1 presents measurements details of the specimens.

Table 1: Specimens Measurements.

Sample	1	2	3	4	5	6
d (mm)	0	2	4	6	8	0
t (mm)	3.1	3.1	3.1	3.1	3.1	3.1
w (mm)	22.5	22.5	22.5	22.5	22.5	22.5
L (mm)	100	100	100	100	100	100

The experimental tests were performed by subjecting each of the specimens to unidirectional tensile test in an Instron 3369 universal testing machine, programmed to collect data of load and displacement at the rate of 5 Hz. During the tests, a camera captured images of the specimens at the rate of 1 picture/s. These images were processed in the software VIC-2D, from Correlated Solutions, providing local strain fields for each image of the tests.

2.1 Material's Characterization

Through the data collected from the un-notched specimens tests, 1 and 6, and the equations (1) to (3), it was possible to develop the Stress x Strain curve of the material and its strain field for the ultimate strength (σ_N). Applying the theoretical approach to homogeneous material to those results makes it possible to extract the mechanical properties of the material: Tensile Strength (σ_0), from the maximum value of tension during the test; Elastic Modulus (E), from the Stress x Strain curve, considering ($E_x = E_y = E$); Poisson's Ratio (ν_{xy}), from strain data in the principal directions (x and y) and Shear Modulus (G_{xy}), estimated from equation (4).

$$A = w * t \quad (1)$$

$$\sigma_{\infty} = \frac{C}{A} \quad (2)$$

$$\varepsilon_G = \frac{\Delta L}{L} \quad (3)$$

$$G_{xy} = \frac{E}{2(1 + \nu_{xy})} \quad (4)$$

where A is the cross-sectional area of the specimen, σ_{∞} is the applied stress, C is the applied load, ε_G is the global strain, ΔL is the displacement of the load cell.

2.2 Influence of the Hole in the Material's Strength

The influence of the presence of the hole and its diameter in the strength of the material was analysed using the data collected directly from the tension tests, generating graphics of Load x Displacement. To analyse the influence in tension terms, the equation (5) was applied in the generation of Notched Tensile Strength x Diameter graphics.

$$\sigma_N = \frac{C_{max}}{A} \quad (5)$$

To evaluate the reliability of the data collected from the tests, they were compared to the the models proposed by Martins *et al.*, based on the analytical predictions made by Whitney-Nuismer and Mar-Lin [10].

Whitney and Nuismer proposed two methods: the Point Stress Criterion, equation (6), and the Average Stress Criterion, equation (7). The first one proposes that the failure of the material occurs when the stress at a distance d_0 ahead of the hole edge reaches the un-notched

material strength (σ_0); the second one, proposes that the failure occur when the average stress over a distance a_0 ahead of the hole edge reaches the un-notched material strength (σ_0) [11].

$$\frac{\sigma_N}{\sigma_0} = \frac{2}{2 + \varphi^2 + 3\varphi^4 - (k_\sigma - 3)(5\varphi^6 - 7\varphi^8)} \quad (6)$$

$$\frac{\sigma_N}{\sigma_0} = \frac{2(1 - \phi)}{2 - \varphi^2 - \varphi^4 + (k_\sigma - 3)(\varphi^6 - \varphi^8)} \quad (7)$$

where k_σ is the stress concentration factor for an anisotropic infinite plate with a hole, given by equation (8), and φ and ϕ , given by equations (9) and (10) respectively, are defined for simplification of calculus as functions of the hole radius (R).

$$k_\sigma = 1 + \sqrt{2 \left[\frac{E_x}{E_y} - \nu_{xy} \right] + \frac{E_x}{G_{xy}}} \quad (8)$$

$$\varphi = \frac{R}{R + a_0} \quad (9)$$

$$\phi = \frac{R}{R + d_0} \quad (10)$$

The characteristics lengths a_0 and d_0 represent distances ahead of the hole edge and are determined through the best fit of the curves with the experimental results.

While these Whitney-Nuismer criterions consider the composite as a homogeneous material, Mar-Lin's consider the application and the behaviour of all the composing materials. This criterion propose that the failure occur after a cracking in the interface between the resin and the fibers [10]. Using properties like the hole diameter (d), the laminate fracture toughness (H_C) and the power of singularity (m), it defines:

$$\frac{\sigma_N}{\sigma_0} = \frac{H_C(d)^{-m}}{\sigma_0} \quad (11)$$

where H_C and m are properties of the material, defined through the best fit of the curves with the experimental results in a $\log(\sigma_N/\sigma_0) \times \log(d)$ domain.

2.3 Influence of the Hole in the Material's Local Strain Profile

The influence of the hole presence and diameter in the local strain was obtained through analysis of the data collected using the DIC method. It was possible to calculate data of local strain in the direction of the applied load (ϵ_{yy}) over the crack axis in notched strength condition. Figure 2a shows the profile expected for the deformation field.

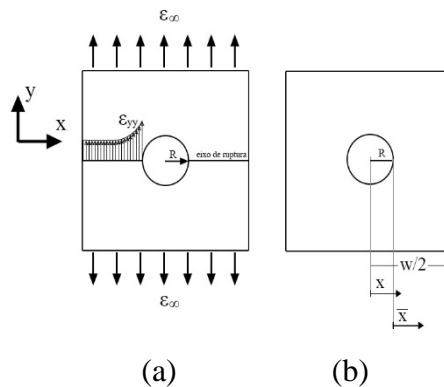


Figure 2: (a) Expected deformation field and (b) Dimensions of the specimen used as reference to equation (12).

To analyse the deformation along the half-width of each specimen in increasing load, data of $(\epsilon/\epsilon_{\infty})$, from the deformation fields, was crossed with a dimensionless length (\bar{x}), defined by equation (12) and Figure 2b.

$$\bar{x} = \frac{x - R}{w/2 - R} \quad (12)$$

3. RESULTS AND DISCUSSION

Data collected from the un-notched specimens tests could not be used on the failure analysis, since their failure occurred in the clamp region, out of the camera's field of capture, but their load and strain data were very useful in the characterization of the material. On the other hand, the failure of the notched specimens occurred at the expected region: over x axis, crossing the center of the hole. Pictures of the specimens before and after the tests are presented in Figure 3.

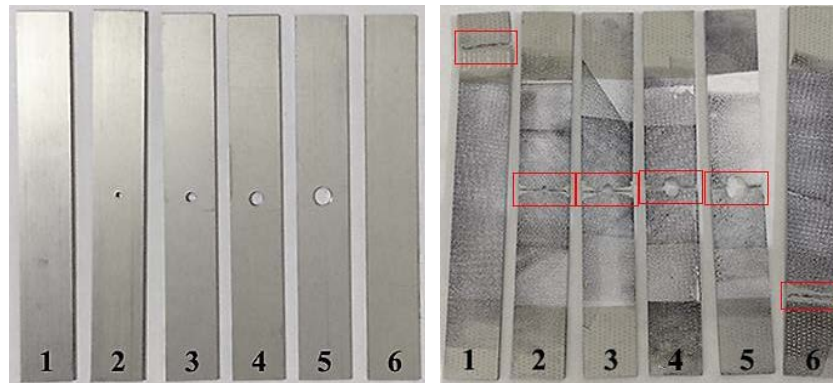


Figure 3: Specimens before and after the tests with fracture regions highlighted.

3.1 Material's Characterization

The material's properties, defined using data from the un-notched specimens tests are presented in Table 2.

Table 2 : Material Properties Values.

σ_0 (Mpa)	E (MPa)	ν_{xy}	G_{xy} (MPa)
448.80	12333.55	0.1982	5146.71

3.2 Influence of the Hole in the Material's Strength

Through the Load x Displacement curves, Figure 4, we can note that the hole diameter significantly affects the mechanical capacity of the material under tension. This reduction in its capacity is highlighted in Figure 5, in which it is possible to note that the Ultimate Strength exponentially decreases with the increasing of the hole diameter.

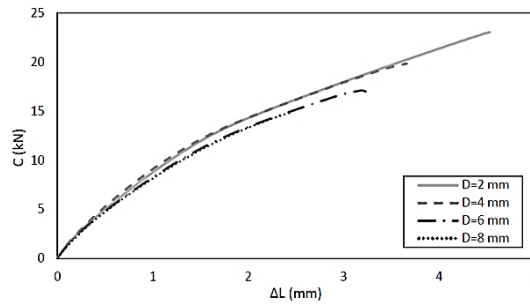


Figure 4: Relation between Load and Displacement for each hole diameter.

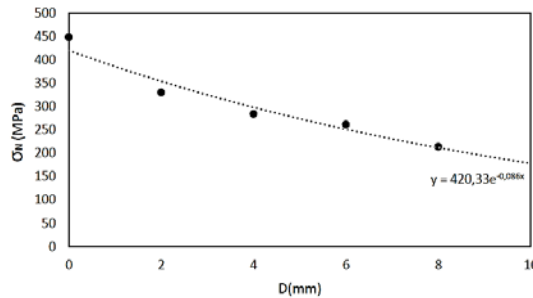


Figure 5: Ultimate Strength for each diameter tested and tendency curve.

The verification of the data reliability, made through comparison to Whitney-Nuismer and Mar-Lin criterions, provided great results. Figure 6 shows that the experimental results fit the curves with small disturbance, especially to the one related to Mar-Lin's criterion, probably because this is the one that take in account the non-homogenous character of the material. The only point that haven't corresponded to the theoretical prediction was the one of greatest diameter, in this case two stress concentration factors, the hole's edges and the specimen edges, were too close to each other, compromising the deformation capacity of the material to higher loads.

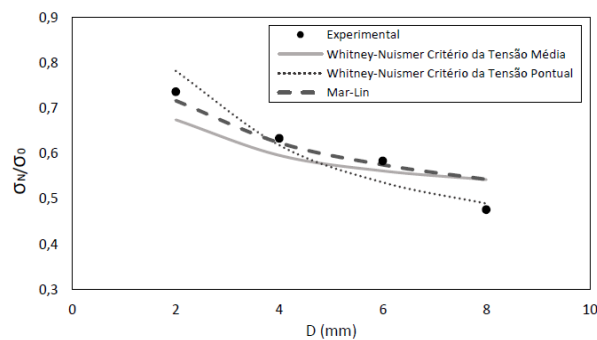


Figure 6: Comparison of the experimental tension ratios to the theoretical ones.

3.3 Influence of the Hole in the Material's Local Strain Profile

The local strain (ϵ_{xy}) analysed over the failure axis for notched tensile strength conditions, presented in Figure 7, indicates greater strain closer to the holes edges, as expected. The local strain of the specimen of 8 mm diameter deformed less than the others specimens, because of the proximity between the hole's edges and the specimen's edges.

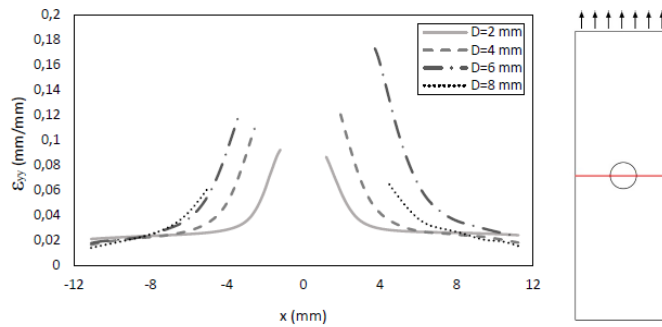


Figure 7: Maximum local strain over the failure axis.

The strain fields (Figure 8) show regions of greater strains, indication of tension (in red), and regions of smaller strains, indication of compression (in blue and pink). It is also possible to note that those tension regions develop in “X” form, indicating good stress transference by the fibers at 0°/90°.

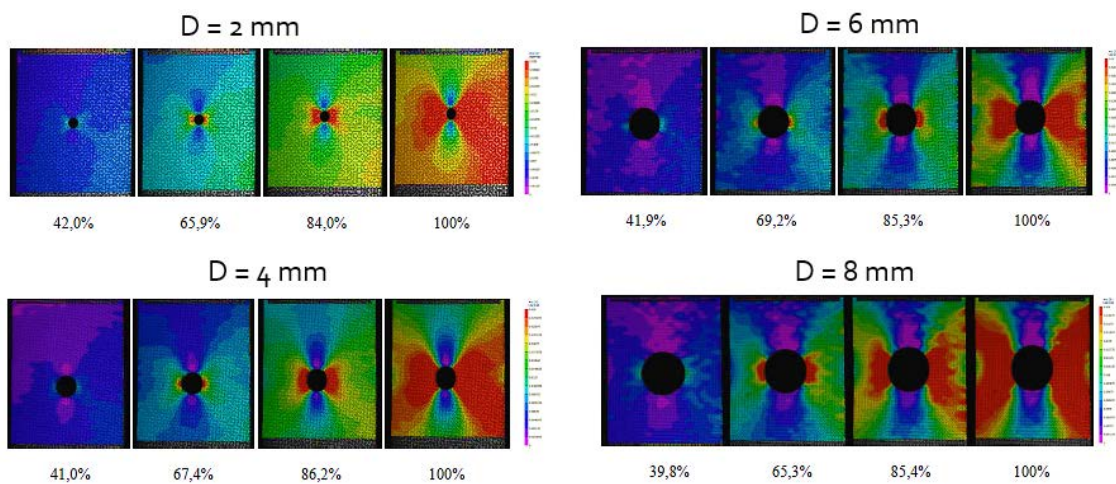


Figure 8: Strain fields presented in percentage of Notched Tensile Strength ($\% \sigma_N$).

Analysing the tension regions in terms of \bar{x} length under some conditions of tension, Figure 9, it is possible to verify that: before the failure the curves tend to ratio 1 in the specimen width; the curves that refer to the Notched Tensile Strength indicate lack of width length for the stress condition to normalize. It leads us to conclude that the ideal situation is that the ratio $\epsilon/\epsilon_\infty \rightarrow 1$ in $\bar{x} < 1$ for the maximum operation load of the plate.

The specimen with 8 mm of diameter is, again, an exception, since the stress concentrated in the hole's edges and in the specimen's edges interact with each other, causing the concentration of even greater stresses and resulting in earlier failure.

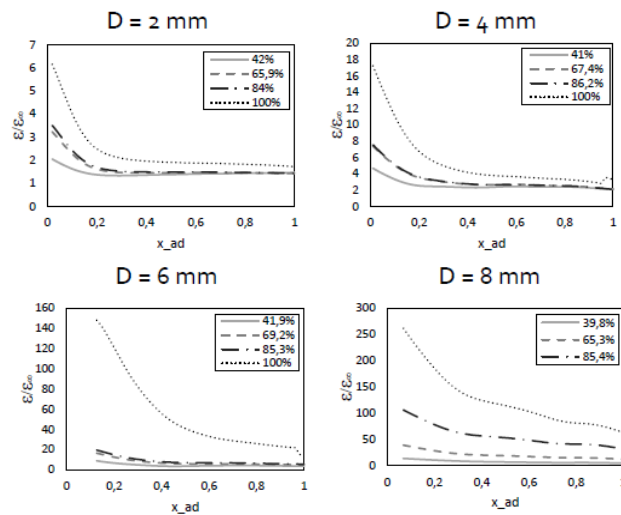


Figure 9: Relation between the strain ratio and the dimensionless length \bar{x} in $\% \sigma_N$.

4. CONCLUSIONS

- The tests complied with theoretical methodologies and generated reliable characterization of the material's mechanical properties;
- The Digital Image Correlation technique has proven to be a simple and quick way to calculate the local strain of the specimens;
- Open-holes significantly reduce the material's plate strength and strain;
- The dimensions of the plate with holes must be defined to ensure that the edges of the holes are distant to other stress concentrator factors;
- Grater displacements in the region of the hole occur in the direction of the fibers and the tension region surrounding the hole in the strain fields develops in the form of "X", both phenomena are indications of the influence of the composite's fibers orientation and tensile transference.

REFERENCES

- [1] Vlot, A., 'Glare: history of the development of a new aircraft material', (Kluwer Academic Publishers, Dordrecht, 2004).
- [2] Vlot, A., Gunnink, J. W., 'Fiber Metal Laminates: An Introduction' (Springer Science+Business Media, Dordrecht, 2001).
- [3] Hwang, W. J., Park, Y. T., Hwang, W., 'Fiber Reinforced Metal Laminates with a Circular Hole' in Metals and Materials International, v. 11 (2005), p. 197-204.
- [4] Sundi, A., Choi, A. Y. N., 'Fiber Metal Laminates: An Advanced Material for Future Aircraft' in Journal of Materials Processing Technology, v. 63 (1997), p. 384-394.
- [5] Megson, T. H. G., 'Aircraft Structures for Engineering Students', 4th edition (Butterworth-Heinemann, Oxford, 2007).
- [6] Carlsson, L. A., Adams, D. F., Piper, R. B., 'Experimental Characterization of Advanced Composite Materials', 4th edition (CRC Press, 2014).
- [7] Dowling, N. E., 'Mechanical Behaviour of Materials – Engineering Methods for Deformation Fracture and Fatigue', 4th edition (PEARSON, 2013).
- [8] Gere, J. M., Goodno, B. J., 'Mechanics of Material', 8th edition (Cengage Learning, 2013).
- [9] Rodi, R., Alderliesten, R. C., Benedictus, R., 'Crack-Tip Behaviour in Fiber/Metal Laminates by Means of Digital-Image Correlation' in Journal of Aircraft, v. 47 (2010), p. 1636-1646.
- [10] Martins, R. D., Donadon, M. V., Almeida, S. F. M. D., 'The Effects of Curvature and Internal Pressure on the Compression-After-Impact Strength of Composite Laminates' in Journal of Composite Materials (2015).

- [11] Whitney, J. M., Nuismer, R. J., 'Stress Fracture Criteria for Laminated Composites Containing Stress Concentrations' in Journal of Composite Materials (1974).